Atomic Scale Modeling of the Effect of Irradiation on Silica Optical Fibers

Harish Govindarajan *, Materials Science Engineering, The Ohio State University

Introduction

Optical fibers and optically-based sensors find extensive use in instrumentation and control systems in nuclear power plants due to their desirable characteristics and advantages over traditional electrical transmission systems, such as immunity to electromagnetic interference (EMI) [1]. Vitreous silica which has a high melting point (~1650°C), is a suitable material for optical fiber and sensor applications within high-temperature reactor pressure vessels. However, although pure vitreous silica-core fibers are transparent over a broad spectrum (ultraviolet to near infrared), irradiation causes the optical fibers to "darken" and form "color centers" [2]. This leads to preferential absorption of light at frequencies specific to the defect type, resulting in the attenuation of signals, and is a major concern for these applications. While abundant experimental information exists on the various defects in silica and their corresponding optical properties [3], there still needs to be an accurate and predictive modeling approach that can provide useful information about defect evolution in the structure and crystallization effects upon heating and irradiation, and establish the correlation between the local structural defects caused by irradiation to optical transmission losses over typical lengths of the fiber. This paper presents a computational approach using (a) molecular dynamics calculations to simulate irradiation damage, (b) a set of techniques to extract and correlate the structural defects thus created [4], and (c) ab-initio electronic structure calculations with Hybrid Density Functional Theory (DFT) methods to model the effect of the structural defects on the electronic and optical properties [5].

*Collaborators: Rohan Mishra & Dr. Wolfgang Windl, The Ohio State University

Modeling Methodology

Molecular Dynamics Simulations

We used molecular dynamics simulations using the LAMMPS package [6] to simulate the irradiation damage in amorphous silica. The Munetoh-Tersoff inter-atomic potential [7] was identified as the best compromise between computational efficiency and accuracy and was used for our calculations. The vitreous silica network, formed by silicon atoms tetrahedrally bonded to oxygen atoms, has a short-range order very similar to beta-cristobalite. In order to build the amorphous silica network, we melted the beta-cristobalite structure at 7000 K and subsequently quenched the structure at a rate of 2.4×10^{14} K/s to 3000 K using a Nosé-Hover thermostat. This structure was then annealed using a constant volume, constant temperature simulation for 250 ps and subsequently quenched to 300 K at the same rate. The amorphous structure thus formed was analyzed to ensure that the Zachariassen rules for glass formation are met [8]. For simulating the irradiation cascade, we used a simulation box with 81,000 atoms with periodic boundary conditions, and an adiabatic 'skin' near the border of the simulation box held at 300 K. An energetic primary knock-on atom (PKA) was chosen at the center of the simulation cell and the cascade process was integrated with a varying time-step in the range of 0.001 fs to 0.1 fs up to a total time of 4 ps. A range of energies between 0.5 and 4 keV based on literature and experiments were used for the initial energy of the PKA atom.

Results from MD Simulations

After sufficient time evolution, the irradiated system is quenched to room temperature (300 K) and the resulting structure is analyzed for defects. Whereas the identification of optically active defect structures in terms of vacancies or miscoordinated atoms has been established [4], the more general question about what quantities give useful information about structural changes in

the structure and crystallization effects upon heating and irradiation required examination of a large number of approaches discussed in the literature [9] and known from experimentation until a solution satisfactory for our purposes had been found. We have identified a set of techniques that allow us to analyze the data from MD simulations and also to connect the findings to literature and experimental results.

Ring-order distribution

After MD simulations of irradiation events, four types of defective bonding are primarily observed, namely Si5, Si3, O1, O3 - where the number indicates the coordination of the atom. Besides miscoordination, the amorphous network was changed in a more global way as seen in the length distribution of closed ring paths that lead from a Si-atom along Si-O bonds back to itself [9], which we calculate using a "Depth-First Traversal" algorithm. Rings of order 3, 4, 5 and 6 are observed in the structure with the ring distribution centered at 6-member rings at room temperature, in conformity with existing MD studies in literature [9, 10]. Within the 1400 K temperature range, there is an increase in the percentage of 3 and 4 member rings followed by a decrease in the percentage of 6 member rings (Figure 1). The preliminary irradiation analysis with a PKA energy of 4 keV also indicates a higher increase in the percentage of 3 and 4 member rings and a decrease in the percentage of 6 member rings. As established in literature, 3 member rings are very close to planar rings and correspond to the vibrational frequencies of D1 and D2 lines detected by Raman Spectroscopy [11], which thus allow experimental validation.

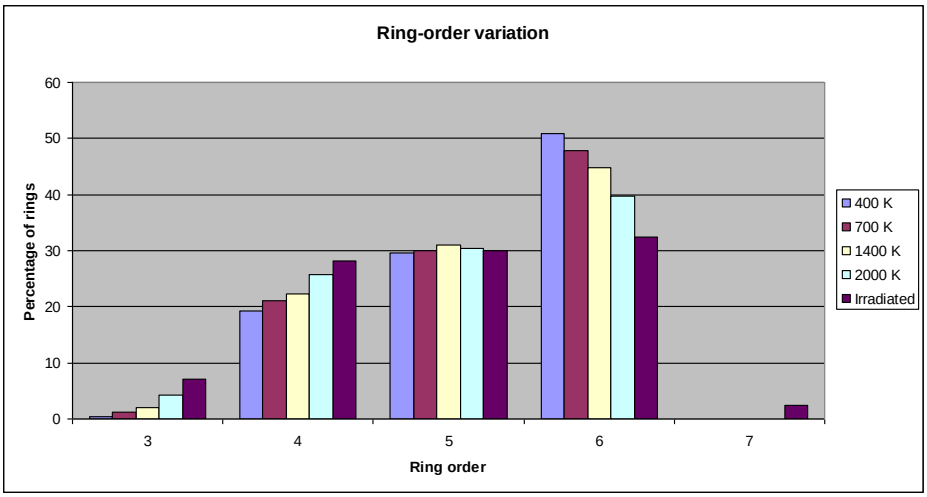

Figure 1: Variation of ring size with temperature and irradiation.

Pair-correlation functions & Structure Factor

Pair-correlation functions of Si-Si, O-O, and Si-O pairs are determined for varying temperatures and compared. A decrease in peak height with rising temperature can be observed (Figure 2), while the peak positions remain unchanged. This corroborates previous work suggesting that the thermal expansion in amorphous silica is not dominated by changes in the nearest-neighbor bond lengths but by the deformation of network-forming rings described earlier [12].

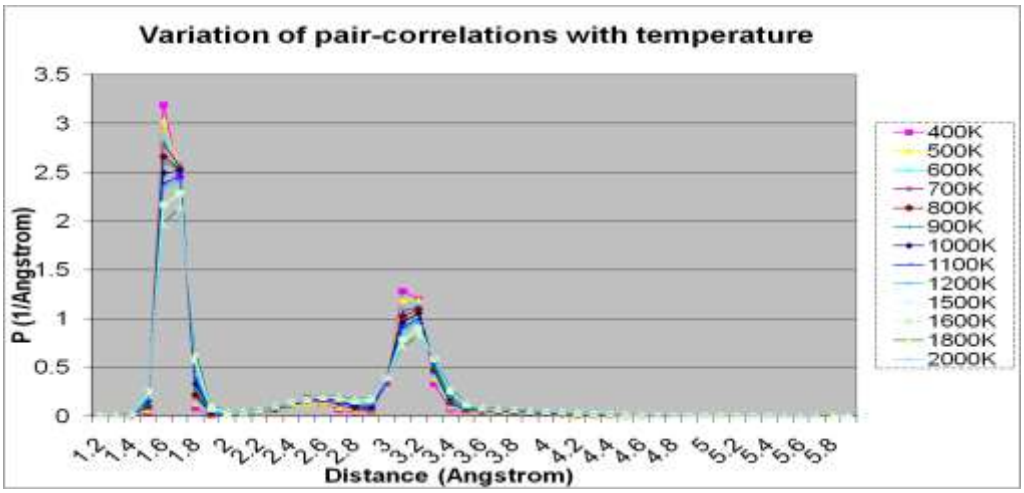

Figure 2: Variation of pair-correlation function with temperature.

The Structure factor, obtained as a function of the Fourier transform of the radial distribution function, is computed and compared between the irradiated structure and the pristine structure at room temperature. The structure factor, which provides information about the medium range order of amorphous materials, can be measured experimentally through x-ray or neutron diffraction. The comparison of structure factor of the irradiated structure and the relaxed structure reveals a relative decrease in the height of the peaks obtained (Figure 3). The relative decrease in structure factor and the increase in percentage of small (3 & 4) member rings with irradiation motivated us to explore the possibility of recyrstallization in the material with irradiation.

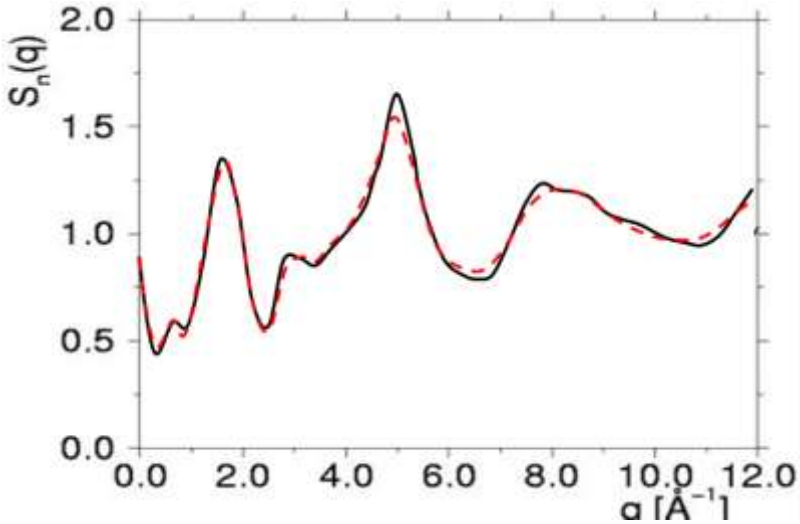

Figure 3: Structure factor of the initial amorphous structure (black solid line) and MD simulations of irradiated structure using a PKA energy of 4 keV (red dashed line).

X-ray diffraction simulation

The Crystal Diffract tool in the Crystal Maker package is used to simulate an XRD analysis of the structures. A Gaussian interpolation is used to plot the diffraction data where the symmetry and shape of the peaks give an indication of the relative crystallization of the structure. The instrumental broadening parameter is kept at the default value of 9.509^{o}. XRD spectra are obtained for beta-crystobalite silica, amorphous silica at room-temperature and irradiated silica

quenched to room temperature (Figure 4). From the XRD data of crystalline beta-cristobalite, a number of distinct peaks are observed corresponding to the planes producing reflections. The amorphous silica structure at room temperature produces a near-symmetrical peak at around 21^{o} with a slight hump at 9.5^{o}. The irradiated structure, when analyzed, produces a second characteristic peak at 44^{o} in addition to the peak at 21^{o}. This indicated the possibility of a partial crystallization of the structure and corresponds to the peaks seen in the crystobalite spectrum.

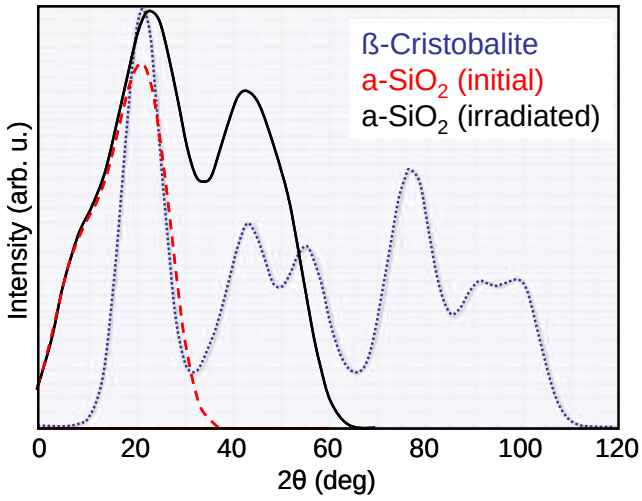

Figure 4: XRD Gaussian-fit data of crystalline beta-cristobalite (blue dotted line) and amorphous SiO_2 before (red dashed line) and after 4 keV knock-on event (black solid line) for modeled structures using Crystal Diffract.

Electronic structure calculations

Methodology

The electronic and optical properties of defective oxygen vacancy configurations identified from the MD simulations of the irradiated silica structure were calculated using hybrid Density Functional Theory (DFT) methods with the Vienna Ab-Initio Simulation Package (VASP) [13]. Since electronic structure calculations in VASP are not computationally efficient for large simulation cells, a method to isolate the defects in the large irradiated structure was developed. A

48-atom simulation cell was defined individually around the various defective oxygen vacancy configurations in the irradiated structure and extracted such that a single oxygen vacancy was present in each extracted cell. Beginning with a 48-atom simulation cell of cubic crystalline beta cristobalite structure, MD simulations were performed with a NVE thermostat to heat the structure, starting from 300 K to 1000 K. Structural parameters, such as RDF and bond lengths of the evolving beta-cristobalite cell were continuously monitored until they matched the defective configurations of the irradiated structure within a tolerance of 0.1%. Preliminary electronic structure calculations for the perfect and oxygen vacancy configuration of beta-cristobalite were performed with a 4x4x4 k-point mesh. Since DFT with traditional local and semilocal functionals are generally known to underestimate the band gaps of bulk semiconductors and insulators, the HSE hybrid functional, which typically gives a more accurate result of the band gap by including just the significant parts of the exact nonlocal Hartree–Fock-type exchange, was used for the calculations [14].

Results of Electronic Structure Calculations

The density of states of the perfect and oxygen vacancy configurations of beta cristobalite were calculated. An atomic-exchange parameter of 0.35 in the HSE functional yields a band gap of 8.04 eV for beta-cristobalite silica, which compares well with photoconductivity measurements in literature [15]. Additional states in the density of states calculation (Figure 5) arise due to the change in the electronic structure of irradiated silica arising from the defective oxygen vacancy configuration. This corresponds to a change in the electronic energy band structure and optical absorption coefficient of irradiated silica.

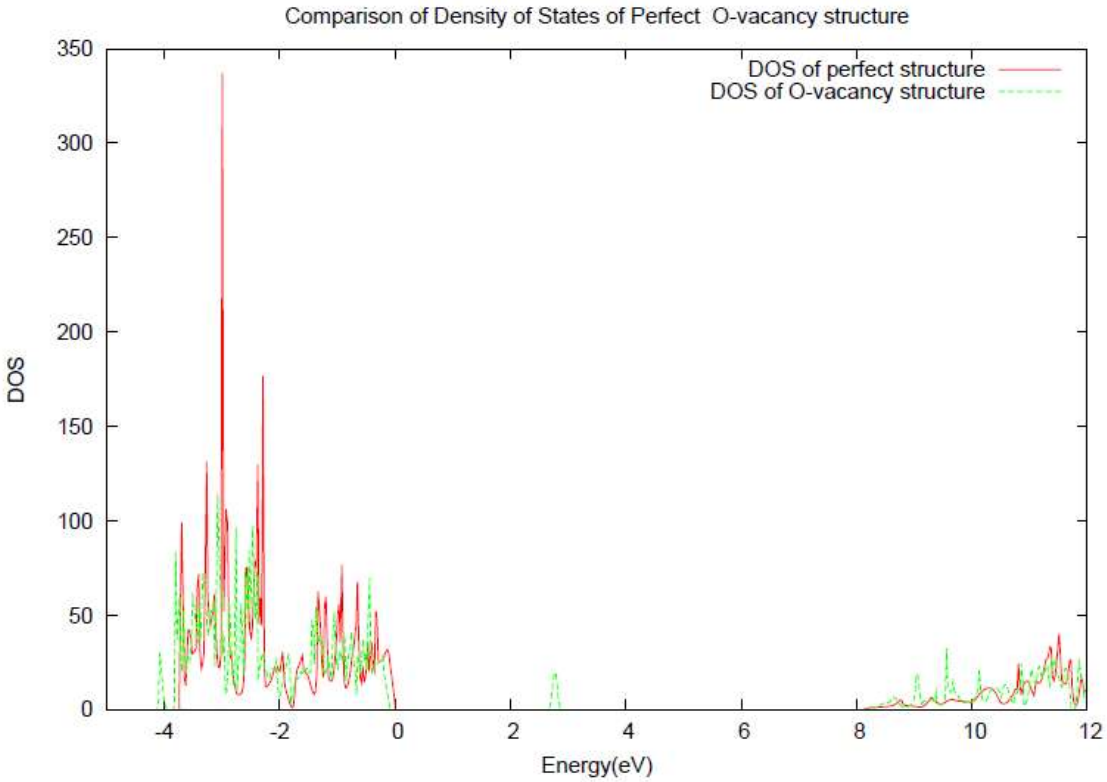

Figure 5: Comparison of density of states of perfect structure and defective oxygen vacancy structure of beta-cristobalite.

Absorption Coefficient

The absorption coefficient corresponding to the defective oxygen vacancy configuration in beta-cristobalite silica is calculated and plotted (Figure 6). Prominent changes in the absorption for the defective configuration are observed within the energy range of 5.8 to 9.5 eV with a maximum value centered at 6.20 eV. This compares well with existing literature [17] and is attributed to the transition between the occupied and unoccupied defect states arising from the defective oxygen vacancy configuration.

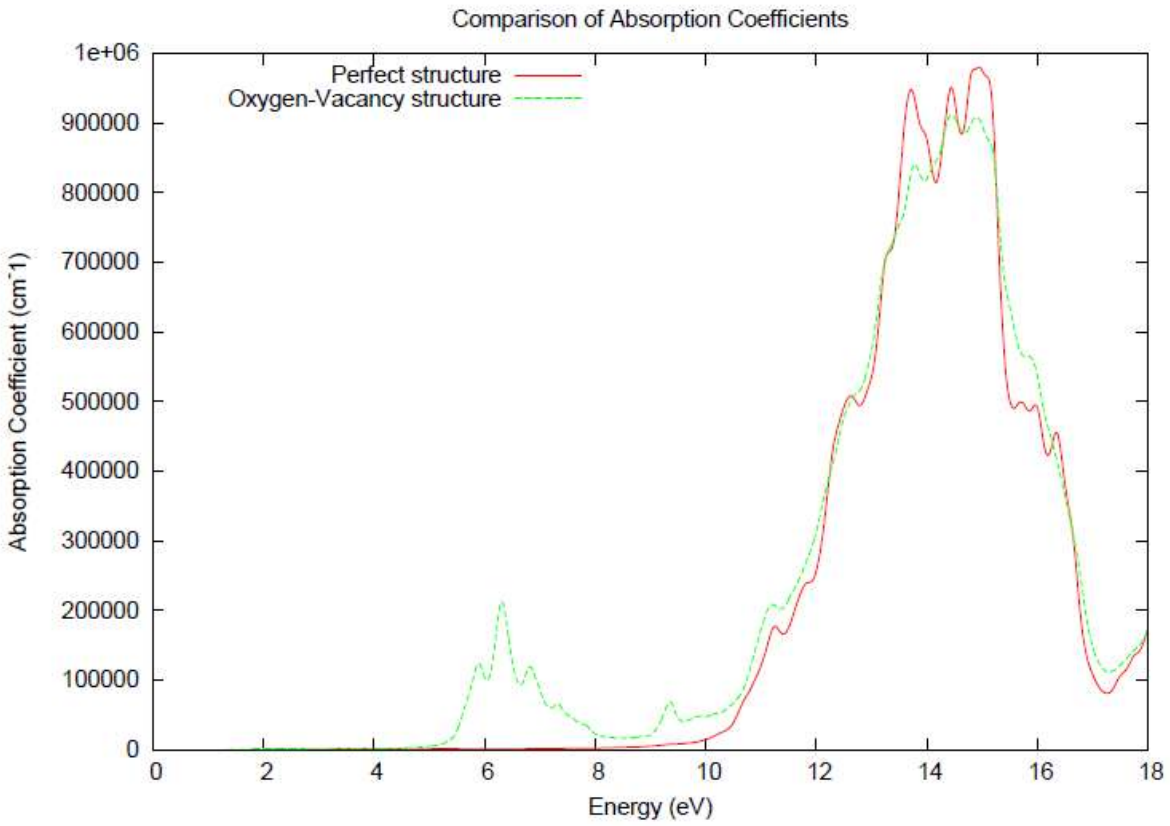

Figure 6: Comparison of absorption coefficients of perfect and defective oxygen vacancy beta-cristobalite structures.

Conclusions

This paper presents a computational approach to simulate irradiation damage, using molecular dynamics calculations and to identify structural parameters that provide useful information about structural changes in the structure and crystallization effects upon heating and irradiation. A 'depth-first traversal' algorithm, used to characterize the ring-order distribution of the irradiated structure, indicated a reduction in the higher order rings and an increase in 3 and 4 membered rings upon irradiation. This information, coupled with the reduction in the structure factor and the corresponding peaks of the radial distribution function, besides the additional peak in the X-Ray Difraction simulation of the irradiated structure, indicates the possibility of the presence of crystallization pockets in the irradiated structure. We also performed preliminary first principles DFT calculations using the hybrid HSE functional with an optimized atomic exchange parameter

of 0.35, which gave an accurate value of the band gap. We calculated the density of states and the corresponding absorption coefficient for the defective configuration and found an additional absorption peak centered at 6.20 eV, which compares well with existing literature [17] and was ascribed to additional transitions between the non-defective network states and the defect states.

References

1. "*Fiber Optic Sensors in Nuclear Power Plant Radiation Environments*", Phase 1, EPRI, Palo Alto, CA, Report TR-107326-V1, 1999
2. D. W. Cooke, B. L. Bennett, and E. H. Farnum, "*Optical Absorption of Neutron-Irradiated Silica Fibers*," Journal of Nuclear Materials 232, 214-218, 1996
3. L. Skuja, "*Optical properties of defects in silica*", in: G. Pacchioni, L. Skuja, D. L. Griscom (Eds.), Defects in SiO_2 and Related Dielectrics: Science and Technology, 73–116 Science Series, Kluwer Academic Publishers, 2000
4. F. Mota, M.-J. Caturla, J. M. Perlado, J. Mollá, and A. Ibarra, "*Identification and characterization of defects produced in irradiated fused silica through molecular dynamics",* Journal of Nuclear Materials, Volumes 367-370, 344-349, 2007
5. J. Heyd, G. E. Scuseria, and M. Ernzerhof, "*Hybrid functional based on a screened Coloumb potential*", Journal of Chemical Physics 118, 8207, 2003
6. S. Plimpton, "*Fast Parallel Algorithms for Short-Range Molecular Dynamics*", Journal of Computational Physics 117, 1-19, 1995
7. S. Munetoh, T. Motooka, K. Moriguchi, and A. Shintani, "*Interatomic potential for Si–O systems using Tersoff parameterization*", Computational Materials Science 39, 334–339, 2007
8. W. H. Zachariasen, "*The Atomic Arrangement in Glass*", *Journal of the American Chemical Society, 54*, 3841–3851, 1932
9. F. Mota, M.-J. Caturla, J. M. Perlado, J. Mollá, and A. Ibarra, "*Molecular dynamics study of structure transformation and H effects in irradiated silica*", Journal of Nuclear Materials, 386-388, 75-78, 2009
10. J. P. Rino, G. Gutierrez, I. Ebbsjö, R. K. Kalia, and P. Vashista, Symp. Mater. Res. Soc. Proc. 408, 333 (1996)
11. S. G. Demos, L. Sheehan, and M. R. Kozlowski, Proc. SPIE Int. Soc. Opt. Eng. 3933, 316 (2000)
12. K. Yamahara, K. Okazaki, and K. Kawamura, "*Molecular Dynamics study of the thermal behavior of silica glass/melt and cristobalite*", Journal of Non-Crystalline Solids 291, 32-42 (2001)
13. G. Kresse and J. Hafner, Physical Review B **47** , 558 (1993); ibid. **49** , 14 251 (1994)
14. T. M. Henderson, J. Paier, and G. E. Scuseria, "*Accurate treatment of solids with the HSE screened hybrid.*" physica status solidi (b) 248, 767–774 (2011)
15. T. H. DiStefano and D. E. Eastman, Solid State Communications 9,2259 (1971)
16. L. E. Ramos, J. Furthmüller, and F. Bechstedt, "*Quasiparticle band structures and optical spectra of beta-cristobalite SiO_2*", Physical Review B 69, 085102 (2004)

17. T. Tamura, S. Ishibashi, S. Tanaka, M. Kohyama, and M.-H. Lee, "*First-principles analysis of the optical properties of structural disorder in SiO_2 glass*", Physical Review B 77, 085207 (2008)